A Third Order Central WENO Scheme for 2D Conservation Laws

Doron Levy [a] Gabriella Puppo [b] Giovanni Russo [c]

[a] *Département de Mathématiques et d'Informatique, Ecole Normale Supérieure, 45 rue d'Ulm, 75230 Paris Cedex 05, France; dlevy@dmi.ens.fr*

[b] *Dipartimento di Matematica, Politecnico di Torino, Corso Duca degli Abruzzi 24, 10129 Torino, Italy; puppo@calvino.polito.it .*

[c] *Dipartimento di Matematica, Università dell'Aquila, Via Vetoio, loc. Coppito - 67100 L'Aquila, Italy; russo@univaq.it*

Abstract

We present a new third-order essentially non-oscillatory central scheme for approximating solutions of two-dimensional hyperbolic conservation laws. Our scheme is based on a two-dimensional extension of the centered weighted essentially non-oscillatory (CWENO) reconstruction we presented in [3]. This is a "true" 2D method; it is not based on a direction-by-direction approach. Our method is formalized in terms of a black box which needs as an input only the specific flux. The numerical results we present support our expectations for a robust and high-resolution method.

Key words: Hyperbolic conservation laws, 2D, central difference schemes, high-order accuracy, non-oscillatory schemes, CWENO reconstruction.

1 Introduction

In this work, we present a new third order accurate essentially non-oscillatory scheme for integrating scalar conservation laws in 2D. This scheme is based on the extension to 2D of the one-dimensional Central WENO scheme we presented in [3]. To our knowledge, this is the first 2D non-oscillatory central third order accurate scheme.

The main idea is to use a convex combination of high order interpolating polynomials, as in the WENO reconstruction presented in [5] and [1]. Where large gradients occur, the weights of the convex combination are built to switch automatically to one-sided stencils, preventing the introduction of spurious oscillations generated in the non-smooth stencils.

The reconstruction is built to fit the central set-up (see the review in [6] and references therein). The resulting scheme is a flexible black box tool for integrating conservation laws, since it requires in input only the specific flux. Neither approximate Riemann solvers nor projections along characteristic directions are required.

Due to space limitations, many technical details will be omitted. They will be discussed in [4], together with the extension to hyperbolic systems of conservation laws. Moreover, we have recently verified that it is possible to obtain a fourth order 2D CWENO scheme using bi-quadratic rather than quadratic polynomials as building blocks of our reconstruction. The resulting scheme will also be described in [4].

2 Description of the scheme

We consider the two-dimensional hyperbolic conservation law

$$v_t + f(v)_x + g(v)_y = 0, \tag{1}$$

subject to the initial data, $v(x, y, t = 0) = v_0(x, y)$. For simplicity, consider a uniformly spaced grid; denote by $h := \Delta x = \Delta y$ the mesh-spacing in the x- and y-directions, and let $k := \Delta t$ be the time-step. Moreover, $I_{j,k}$ will be the cell centered around the grid point (x_j, y_k), with sides Δx and Δy. To approximate solutions of (1), we introduce a piecewise-polynomial approximate solution $u(\cdot, \cdot, t)$ at the discrete time levels $t^n = n\Delta t$,

$$u(x, y, t^n) = \sum_{j,k} R_{j,k}(x, y)\chi_{j,k}(x, y), \qquad \chi_{j,k}(x, y) := 1_{I_{j,k}}, \tag{2}$$

where $R_{j,k}(x, y)$ are polynomials defined on the cells $I_{j,k}$. The degree of $R_{j,k}$ is determined by the required order of accuracy of the method; in the following we will consider polynomials of degree 2.

2.1 The time marching scheme

Following [2], we can write an exact evolution equation for u, integrating (1) over the staggered control volume, $I_{j+\frac{1}{2},k+\frac{1}{2}} \times [t^n, t^{n+1}]$:

$$\bar{u}^{n+1}_{j+\frac{1}{2},k+\frac{1}{2}} = \frac{1}{h^2}\int\int_{I_{j+\frac{1}{2},k+\frac{1}{2}}} u(x,y,t^n)\,dydx \tag{3}$$
$$-\frac{1}{h^2}\int_{\tau=t^n}^{t^{n+1}}\left\{\int_{y=y_k}^{y_{k+1}}\left[f\left(u(x_{j+1},y,\tau)\right)-f\left(u(x_j,y,\tau)\right)\right]dy\right\}d\tau$$
$$-\frac{1}{h^2}\int_{\tau=t^n}^{t^{n+1}}\left\{\int_{x=x_j}^{x_{j+1}}\left[g\left(u(x,y_{k+1},\tau)\right)-g\left(u(x,y_k,\tau)\right)\right]dx\right\}d\tau.$$

Here, $\bar{u}_{jk}$ is the cell average associated with the cell I_{jk}, i.e., $\bar{u}_{jk} = \frac{1}{h^2}\int\int_{I_{jk}} u$. The first integral on the RHS of (3) is the cell average at time t^n, $\bar{u}^n_{j+\frac{1}{2},k+\frac{1}{2}}$, computed on the staggered cell $I_{j+\frac{1}{2},k+\frac{1}{2}}$. Given the reconstruction $u(x,y,t^n)$, this term can be computed exactly: it will consists of four terms, involving $R_{j+1,k+1}$, $R_{j+1,k}$, $R_{j,k}$ and $R_{j,k+1}$.

The advantage of the central framework appears in the evaluation of the time integrals appearing in (3). The initial data $u(x,y,t^n)$ is discontinuous along the boundaries of the unstaggered cells $I_{j,k}$. Therefore, the finite speed of propagation of signals of (1) ensures that the solution remains smooth along the lines $(x_j,y_k)\times[t^n,t^n+\Delta t]$ for Δt small enough. These are the edges parallel to the time axis of the staggered control volume $I_{j+1/2,k+1/2}\times[t^n,t^n+\Delta t]$. Thus, we can evaluate the integrals appearing in (3) by a quadrature rule, involving only nodes belonging to these edges. More precisely, we use Simpson's rule to evaluate the time integrals and the following quadrature rule in space for the integrals over the cell boundaries:

$$\int_{x_j}^{x_{j+1}} f(x)dx = \frac{h}{24}\Big[-f(x_{j+2})+13f(x_{j+1})+13f(x_j)-f(x_{j-1})\Big]+O(h^4),$$

In this fashion both quadrature rules involve only nodes on which the approximate solution u is well defined. Note that both quadrature rules are accurate enough even for a fourth order scheme. We still need to predict the mid point-values, $u^{n+1/2}, u^{n+1}$, required in the quadrature rule for the time integrals. Again, we use the smoothness of the numerical solution along the lines $(x_j,y_k)\times[t^n,t^n+\Delta t]$ to consider the sequence of Cauchy problems:

$$\begin{cases} v'_{j,k}(\tau) &= F(\tau,v_{j,k}(\tau)) = -f_x(v(x_j,y_k,t^n+\tau))-g_y(v(x_j,y_k,t^n+\tau)) \\ v_{j,k}(\tau=0) &= u(x_j,y_k,t^n), \end{cases} \tag{4}$$

and we solve them up to $\tau=\Delta t$ with a Runge-Kutta scheme. We then obtain the intermediate values at $t^{n+1/2}$ using the corresponding Natural Continuous Extension (see [7] and [3] for the application of NCE's to the present framework).

Thus, a single application of the RK2 scheme yields the two predicted values:

$$u^{n+1/2} = u^n + \frac{\Delta t}{8}\left(3F^{(1)} + F^{(2)}\right) \qquad u^{n+1} = u^n + \frac{\Delta t}{2}\left(F^{(1)} + F^{(2)}\right), \quad (5)$$

where we have dropped the indeces denoting the grid points. Here $F^{(1)}$ and $F^{(2)}$ are the two approximate Runge-Kutta fluxes. In our case: $F^{(1)} = F(t^n, v^n)$ and $F^{(2)} = F(t^n + \Delta t, v^n + \Delta t F^{(1)})$.

Note that the Cauchy problems appearing in (4) are coupled: the computation of each RK flux $F^{(i)}$ requires the evaluation of the x derivative of f and the y derivative of g at the corresponding intermediate time $t = t^n + c_i \Delta t$, with $c_1 = 0$ and $c_2 = 1$. The predicted point values of $u_{j,k}$ at the time $t^n + c_i \Delta t$ are used to compute $f(u_{j,k})$ and $g(u_{j,k})$. These predicted values of f and g are then used for constructing an interpolant from which the point values of $f_x(u)|_{j,k}$ and $g_y(u)|_{j,k}$ can be computed.

2.2 The 2D Reconstruction

Two types of reconstructions are required:

- *Reconstruction from cell averages.* It occurs at the beginning of each time step.
- *Reconstruction from point values.* This step is needed during the evaluation of the Runge-Kutta fluxes.

Reconstruction from cell averages. The reconstruction is based on a convex combination of interpolation polynomials. Let $P_{jk}(x, y)$ be the interpolation polynomial built on the 3×3 stencil centered around the cell I_{jk}. We require that $P_{jk}(x, y)$ satisfies the five conservation requirements:

$$\frac{1}{h^2} \int\limits_{x_{j+i}-h/2}^{x_{j+i}+h/2} \int\limits_{y_{k+l}-h/2}^{y_{k+l}+h/2} P_{jk}(x - x_j, y - y_k)\, dx\, dy = \bar{u}_{j+i,k+l} \tag{6}$$

for $(i, l) = (-1, 0); (0, 0); (1, 0); (0, -1); (0, 1)$. The sixth constraint is:

$$\partial^2_{xy} P_{jk} = \frac{1}{4 \Delta x \Delta y}(\bar{u}_{j+1,k+1} - \bar{u}_{j-1,k+1} - \bar{u}_{j+1,k-1} + \bar{u}_{j-1,k-1}). \tag{7}$$

The explicit expressions for the coefficients of the polynomial can be easily computed, see [4]. The polynomial $P_{j,k}$ just constructed is enough to yield a third order accurate approximation of the point values of u at the center of the cell and of each of the four integrals on the quarter cells. However, if we chose $R_{j,k}(x,y) = P_{j,k}(x,y)$ the reconstruction would be oscillatory.

To prevent the onset of spurious oscillations, we consider a convex combination of all 9 polynomials defined around and on the cell $I_{j,k}$, namely we consider the polynomials $P_{j+i,k+l}$, $i,l = -1,0,1$. The reconstruction in the (j,k)-th cell is given by:

$$R_{jk}(x,y) = \sum_{i,l=-1}^{1} w_{jk}^{il} P_{j+i,k+l}(x - x_{j+i}, y - y_{k+l}). \tag{8}$$

The weights w_{jk}^{il} will be determined according to accuracy and regularity considerations. Where the solution is regular, w_{jk}^{il} must be chosen in order to attain the highest accuracy. If the solution is not regular around the cell I_{jk}, we want $w_{jk}^{il} \simeq 0$ whenever the polynomial $P_{j+i,k+l}$ might create spurious oscillations. The weights therefore are a key ingredient of the scheme. Following the WENO philosophy (see [1] and [3]) we write:

$$w_{j,k}^{i,l} = \frac{\alpha_{j,k}^{i,l}}{\overline{\alpha}_{j,k}}, \qquad \text{where:} \qquad \alpha_{j,k}^{i,l} = \frac{C^{i,l}}{(\epsilon + IS_{j,k}^{i,l})^p} > 0; \tag{9}$$

here the $C^{i,l}$'s are constants designed to maximize accuracy and ϵ and p are parameters: we have always chosen $\epsilon = 10^{-6}$ (which merely prevents division by zero) and $p = 2$, see [1] and [3]. Finally $\overline{\alpha}_{j,k} = \sum_{i,l} \alpha_{j,k}^{i,l}$ is a normalizing factor. The quantities $IS_{j,k}^{i,l}$ are our multidimensional extension of the smoothness indicators proposed in [1]:

$$IS_{j,k}^{i,l} = \sum_{|\alpha|=1,2} \int_{x_j-h/2}^{x_j+h/2} \int_{y_k-h/2}^{y_k+h/2} h^{2(|\alpha|-1)} (D^\alpha P_{j+i,k+l}(x - x_{j+i}, y - y_{k+l}))^2, \tag{10}$$

where $D^\alpha P$ denotes the derivative of order α of P. These quantities can be easily calculated once the interpolating polynomials $P_{j,k}$ are known, see [4] for details. Such a selection of the smoothness indicators guarantees that in smooth regions $IS_{j,k}^{i,l} = O(h^2)$, while in non-smooth regions $IS_{j,k}^{i,l} = O(1)$, which yields $w_{j,k}^{i,l} \simeq 0$.

Finally the constants $C^{i,l}$ must be determined. Unfortunately, there are no positive constants $C^{i,l}$ to yield a fourth order method. This fact limits the present scheme to third order accuracy. However, we can compute the $C^{i,l}$ that cancel as many terms as possible in the expansion for the truncation error, see [4].

Reconstruction from point values. The approach here is very similar to the previous case. We have different requirements for the interpolating polynomials, namely now we enforce interpolation in the sense of point values: $P_{jk}(x_{j+i}-x_j, y_{k+l}-y_k) = u_{j+i,k+l}$ for $(i,l) = (-1,0); (0,0); (1,0); (0,-1); (0,1)$ and

$$\partial^2_{xy} P_{jk} = \frac{1}{4\Delta x \Delta y}(u_{j+1,k+1} - u_{j-1,k+1} - u_{j+1,k-1} + u_{j-1,k-1}). \tag{11}$$

We use the same smoothness indicators computed during the reconstruction from cell averages. The main difference is that most constants $C^{i,l}$ are zero in this case. Namely, for the x derivative only $C^{i,0} \neq 0$ for $i = -1, 0, 1$, while for the y derivative $C^{0,l} \neq 0$ for $l = -1, 0, 1$. This naturally yields a considerable saving in computing time.

3 Numerical Results

N	Constant weights		C-WENO weights	
	L^1 error	L^1 order	L^1 error	L^1 order
10	0.1570E-01	-	0.8524E-01	-
20	0.2667E-02	2.5580	0.2652E-01	1.6847
40	0.3464E-03	2.9444	0.4181E-02	2.6651
80	0.4386E-04	2.9816	0.4427E-04	6.5613
160	0.5487E-05	2.9989	0.5421E-05	3.0295

Table 1
Linear advection, $T = 1, \lambda = .425$, $\epsilon = 10^{-6}, p = 2$.

We numerically study accuracy using the linear advection problem $u_t + u_x + u_y = 0$. The initial condition is: $u_0(x,y) = \sin^2(\pi x)\sin^2(\pi y)$ on $(0,1)^2$, with periodic boundary conditions. We compute the errors on point values at $T = 1$. The results appear in Table 1, where $\lambda = k/h$.

The scheme with the constant weights corresponds to choosing $w^{i,l}_{j,k} = C^{i,l}$. The results appear in the first column of Table 1. It is clear that in this case we have convergence with third order accuracy. The second column contains data obtained with the full non linear scheme. We see that the non linear scheme is not effective on very coarse grids: this is hardly surprising, since the stencil covers a 5×5 square of cells. The linear and the non-linear schemes become comparable on finer grids. We obtain very similar results with the L^∞ norm, [4].

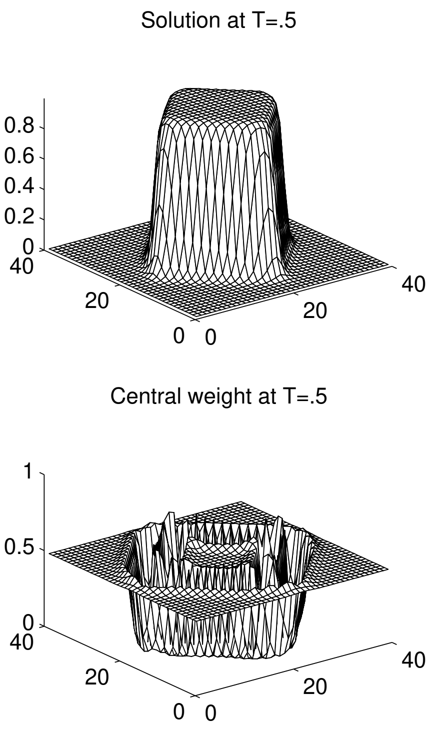

Fig. 1. Linear rotation, $\lambda = .425, h = 1/40$

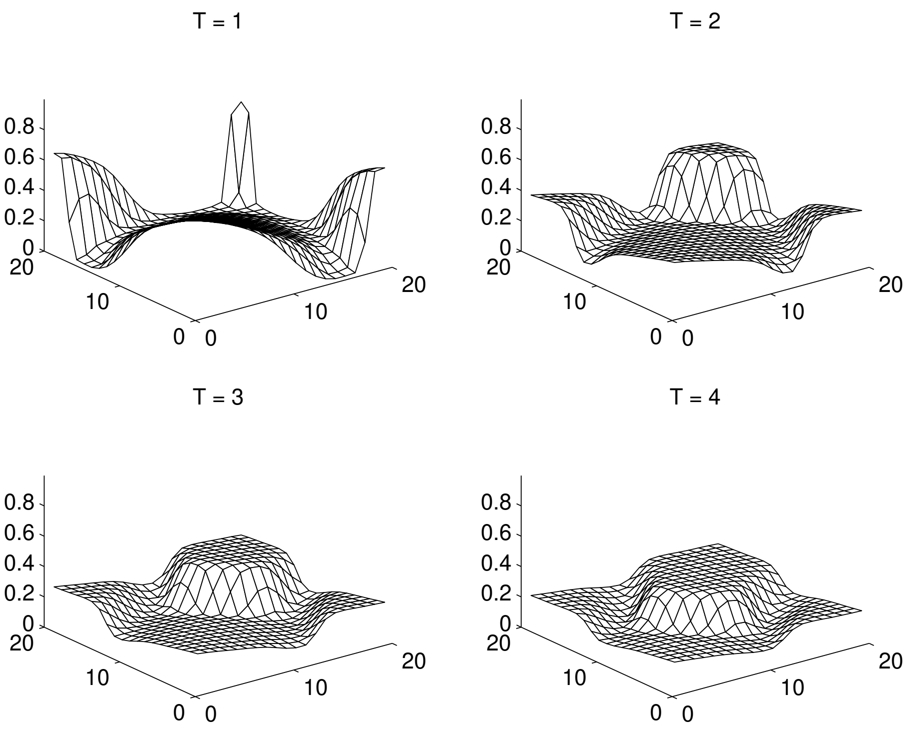

Fig. 2. Burger's equation, $\lambda = .425, h = 1/20$

To demonstrate the effectiveness of the nonlinear weights in preventing the onset of spurious oscillations, we consider the linear rotation of a square patch on $(0,1)^2$, with initial condition $u_0(x,y) = 1$ for $|x-1/2| \leq 1/2$ and $|y-1/2| \leq 1/2$, while $u_0(x,y) = 0$ otherwise. We show the solution after a rotation of $\pi/4$ and $\pi/2$ in Fig. 1. The solution is completely free of spurious oscillations. In the same figure, we also show plots of the corresponding central weight, i.e. $w^{0,0}_{j,k}$. It is clear that $w^{0,0}_{j,k}$ plunges to zero where the numerical solution sharply changes steepness; these are exactly the regions in which the central stencil would yield spurious oscillations, and is therefore assigned an almost zero weight. Even though these discontinuities are linear waves, the resolution is still quite good.

We finally show the results obtained with Burger's equation in Fig. 2. The initial condition is again $u_0(x,y) = \sin^2(\pi x)\sin^2(\pi y)$ on $(0,1)^2$. The fluxes are $f(u) = g(u) = u^2/2$, and we consider periodic boundary conditions. We show the solution up to $T = 4$. Here again we note lack of spurious oscillations, while the shocks are well resolved.

The tests shown are fully 2D problems. In the Burger's test in particular, the solution obtained with the linear weights (not shown here) is so oscillatory that even the propagation speed is highly overestimated. The construction of the 2D weights therefore seems to be both robust and very effective.

References

[1] Jiang G.-S., Shu C.-W., *Efficient Implementation of Weighted ENO Schemes*, JCP, **126**, (1996), pp.202-228.

[2] Jiang G.-S., Tadmor E., *Nonoscillatory Central Schemes for Multidimensional Hyperbolic Conservation Laws*, SIAM J. Sci. Comp., to appear.

[3] Levy D., Puppo G., Russo G. *Central Weno Schemes for Hyperbolic Systems of Conservation Laws*, Math. Mode. and Nume. Anal., in press.

[4] Levy D., Puppo G., Russo G. *Central Weno Schemes for 2D Hyperbolic Systems of Conservation Laws*, in preparation.

[5] Liu X.-D., Osher S., Chan T., *Weighted Essentially Non-oscillatory Schemes*, JCP, **115**, (1994), pp.200-212.

[6] Tadmor E., *Approximate solutions of Nonlinear Conservation Laws*, CIME Lecture notes, 1997, UCLA CAM Report 97-51.

[7] Zennaro M., *Natural Continuous Extensions of Runge-Kutta Methods*, Math. Comp., **46**, (1986), pp.119-133.